



# CHORUS

This is the accepted manuscript made available via CHORUS. The article has been published as:

## Stochastic bifurcations in a prototypical thermoacoustic system

E. A. Gopalakrishnan, J. Tony, E. Sreelekha, and R. I. Sujith

Phys. Rev. E **94**, 022203 — Published 1 August 2016

DOI: [10.1103/PhysRevE.94.022203](https://doi.org/10.1103/PhysRevE.94.022203)

# Stochastic bifurcations in a prototypical thermoacoustic system

Gopalakrishnan, E. A.\* and Tony, J., Sreelekha, E. and Sujith, R. I.

*Department of Aerospace Engineering, IIT Madras, Chennai, India*

(Dated: July 12, 2016)

We study the influence of noise in a prototypical thermoacoustic system, which represents a nonlinear self-excited bistable oscillator. We analyze the time series of unsteady pressure obtained from a horizontal Rijke tube and a mathematical model to identify the effect of noise. We report the occurrence of stochastic bifurcations in a thermoacoustic system by tracking the changes in the stationary amplitude distribution. We observe a complete suppression of bistable zone in the presence of high intensity noise. We find that the complete suppression of bistable zone corresponds to the non-existence of P-bifurcations. This is the first study in thermoacoustics to identify the parameter regimes pertinent to P-bifurcation using the stationary amplitude distribution obtained by solving the Fokker-Planck equation.

## I. INTRODUCTION

Many natural and engineering systems are nonlinear in nature and display bifurcations for suitable change in any of the system parameters. Often, these bifurcations can result in detrimental consequences in a real system. Especially Hopf bifurcation, where the system transitions from a non-oscillatory state to an oscillatory state, is found to be undesirable in many real systems [1, 2]. The effect of noise on the dynamics of these nonlinear systems cannot be neglected as most real systems are noisy. Noise acts as another bifurcation parameter as it can shift bifurcation thresholds [3], induce oscillations [4–6] and introduce novel dynamical states [7]. The noise present in a real system could be independent or dependent on the state of the system. Further, the noise could also be uncorrelated or correlated in nature. It is often difficult to establish the exact nature of noise in a real system. This difficulty brings in the necessity of investigating the effect of noise in mathematical models of real systems along with physical experiments.

The accurate determination of the bifurcation point is nearly impossible in the presence of noise. This difficulty in determining the bifurcation point is because the measured observable is no longer a deterministic quantity but a stochastic variable. Thus a single realization that we obtain in an experiment or from a mathematical model is incapable of providing the complete information about the state of the system. In the presence of noise, stochastic differential equations (SDEs) are adopted instead of ordinary differential equations to describe the evolution of the system. Hence, we need to calculate the probability density function of the observable rather than its absolute value in the presence of noise. The probability density function of a stochastic variable can be obtained by solving the Fokker-Planck equation associated with the SDE [8–10].

As against the deterministic bifurcation where we track the evolution of the absolute value of the observable,

we track the change in the probability distribution of the observable in the presence of noise. The qualitative changes observed in the probability distribution of the observable are termed as phenomenological bifurcations (P-bifurcation). Bifurcation associated with the change in sign of the largest Lyapunov exponent is termed as dynamic bifurcation (D-bifurcation). Both P and D-bifurcations are classified as stochastic bifurcations [11]. There are studies on the effect of additive and multiplicative noise on stochastic bifurcations that happen in nonlinear systems. Additive noise does not change the location of the extrema of the stationary probability density function whereas multiplicative noise can shift the extrema of the distribution [7].

The phenomenon of stochastic bifurcation is very well studied using models. The stochastic Hopf bifurcation is studied in the context of various nonlinear oscillators [1, 7, 12] and in biological systems including neuron models, synthetic gene oscillators [1, 13] and cellular networks [14]. The framework of stochastic bifurcation is also used to study the effect of noise in self-sustained bistable oscillators [1]. Further, there are several experimental studies on stochastic bifurcation in nonlinear systems [15, 16].

The literature on stochastic bifurcation in engineering systems is minimal. Many engineering systems are nonlinear and most engineering systems work in the presence of noise. Due to the nonlinear nature, they can undergo sudden transitions from a non-oscillatory state to an oscillatory state for an infinitesimal change in any of the system parameters. The oscillatory state following a Hopf bifurcation can cause a total collapse or decrease in performance of an engineering system [17]. One such engineering system where the margins of safe operation are limited by Hopf bifurcation is a thermoacoustic system [18]. A thermoacoustic system is a self-excited system where a heat source is located in a confinement or duct [19, 20]. Many power generating systems such as gas turbine engines, industrial burners and aircraft engines belong to the category of thermoacoustic systems. A positive feedback established between the unsteady heat release rate and the inherent fluctuations of the acoustic field present in the duct could result in a Hopf bifurcation. From the literature, it can be seen that thermo-

---

\* Corresponding author.

Email: gopalakrishnanea82@gmail.com

oustic systems often undergo subcritical Hopf bifurcation. Thermoacoustic system which undergoes subcritical Hopf bifurcation is often modeled as a self-sustained bistable oscillator [21–23].

As most of the thermoacoustic systems work in the presence of noise, the effect of noise on the dynamical states of a thermoacoustic system becomes an important topic of study. The presence of noise can transition the thermoacoustic system from non-oscillatory state to oscillatory state when the system is in the bistable regime. There are several experimental [24, 25] and numerical studies [26, 27] on the influence of noise in thermoacoustic systems. Recently, Gopalakrishnan & Sujith [23] performed a study on horizontal Rijke tube in order to understand the effect of noise on the hysteresis characteristics. They performed experiments and adopted a mathematical model to achieve this objective. They found that the width of the bistable zone decreases with increase in the intensity of noise. Moreover, they also reported that there is a suppression of the bistable zone in the presence of high intensity noise. Therefore, it is evident from the results reported by Gopalakrishnan & Sujith [23] that the bifurcation point cannot be ascertained. This difficulty in identifying the Hopf and fold points in the presence of high intensity noise brings in the need to calculate the stationary probability density function of the measured observable. As mentioned earlier, the stationary probability density function can be calculated by solving the Fokker-Planck (FP) equation of the system. Noiray & Schuermans [28, 29], in their pioneering work, introduced Fokker-Planck formalism in the thermoacoustic literature. They derived the FP equation for a thermoacoustic system undergoing supercritical Hopf bifurcation. Their primary focus was to derive growth and decay rates of thermoacoustic oscillations for the unsteady pressure data obtained from a gas turbine engine and compare it with the numerical model.

In summary, the influence of noise characteristics on noise induced transitions has been studied in thermoacoustic systems. The FP equation has been derived for a thermoacoustic system depicting supercritical Hopf bifurcation. The amplitude distribution obtained as a solution to the FP equation has been used to calculate the growth and decay rate of oscillations. The suppression of bistable zone in the presence of high intensity noise is also observed both in experimental and numerical frameworks. However, the issue of identifying the critical points of transition remains to be explored. The amplitude distribution must be adopted instead of the absolute value of the amplitude to determine the transition. In this study, we adopt the concept of stochastic bifurcation to study the effect of noise in a thermoacoustic system. We study the influence of noise in experiments on Rijke tube and in a mathematical model. The model proposed by Balasubramanian & Sujith [21], which depicts subcritical Hopf bifurcation, is used in this study. We derive the stationary amplitude distribution from the FP equation corresponding to the governing equations described

by the model. We identify the parameter regimes corresponding to P-bifurcation in the system.

## II. EXPERIMENTAL SETUP AND MATHEMATICAL MODEL

A horizontal Rijke tube with an electrically heated wire mesh is used to perform the experiments. The schematic of the setup is shown in Fig. 1. The tube is of square cross-section and 1 m long. The cross-sectional area of the duct is  $93 \times 93 \text{ mm}^2$ . A blower (1 HP, Continental Airflow Systems, Type-CLP-2-1-650), operated in the suction mode, is used to provide the mean flow. The flow rate is measured using a compact orifice mass flow meter (Rosemount 3051 SFC). A rectangular chamber of dimensions  $120 \times 45 \times 45 \text{ cm}^3$ , referred to as decoupler, is located at the outlet end of the Rijke tube to reduce the acoustic interactions between the blower and the duct. The decoupler maintains the pressure fluctuations to be zero at that end. A DC power supply unit (TDK-Lambda, GEN 8-400, 0-8 V, 0-400 A) provides the necessary electrical power to the wire mesh. A mesh type electric heater is used because it can supply high amount of electric power for a fairly long duration without any significant structural deformation [30].

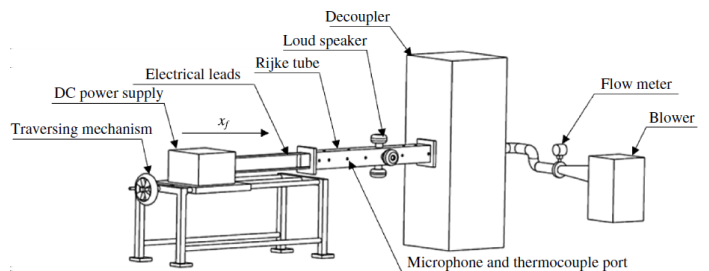


FIG. 1. The schematic of the experimental setup. This figure is reproduced with permission from Ref.[23]. Copyright 2015 Cambridge University Press.

The measurement system consists of a pressure transducer (or a microphone) PCB103B02 connected to a PCI 6221 data acquisition card to record the acoustic pressure and a K-type thermocouple to measure the steady state temperature. The sensitivity of the pressure transducer is  $217.5 \text{ mV kPa}^{-1}$ , the resolution is  $0.2 \text{ Pa}$  and uncertainty is  $\pm 1 \%$  of the reading. The pressure data was acquired at a sampling frequency of  $10 \text{ kHz}$  for 3 seconds. Loudspeakers (Ahuja AU 60) are used to apply external noise. Gaussian white noise is generated using LabVIEW Signal Express and is input to a loudspeaker through an amplifier. More details on the experimental setup can be found in Gopalakrishnan & Sujith [23].

We use a simple nonlinear model that depicts the bistable behavior observed in experiments on horizontal Rijke tube. A modified form of the model developed by Balasubramanian & Sujith [21] is used in this study. To develop this model, the non-dimensional momentum and

energy equations are linearized neglecting the effect of mean flow [31] and temperature gradient. The linearized equations of momentum and energy for the acoustic field are:

$$\gamma M \frac{\partial u'}{\partial t} + \frac{\partial p'}{\partial x} = 0 \quad (1)$$

$$\frac{\partial p'}{\partial t} + \gamma M \frac{\partial u'}{\partial x} = \dot{Q}' \quad (2)$$

where  $\gamma$  is the ratio of specific heat capacities,  $M$  is the mean flow Mach number and  $\dot{Q}'$  is the fluctuating heat release rate. This set of partial differential equations (Eqs. 1 & 2) can be converted to ordinary differential equations through Galerkin expansion [32]. In this expansion, the pressure ( $p'$ ) and velocity ( $u'$ ) fluctuations are expressed as a combination of the basis functions in the domain. Any linearly independent set of functions that satisfy the boundary conditions can be chosen as the basis functions. The pressure ( $p'$ ) and velocity ( $u'$ ) fluctuations can be expressed in terms of the acoustic modes as follows:

$$u' = \sum_{j=1}^{\infty} \eta_j(t) \cos j\pi x, \quad p' = - \sum_{j=1}^{\infty} \frac{\gamma M}{j\pi} \dot{\eta}_j(t) \sin j\pi x \quad (3)$$

The heat release rate fluctuation is modeled as a function of the velocity fluctuations.

$$\dot{Q}' = \dot{Q}'(u'_f(t - \tau)) \quad (4)$$

Here,  $\tau$  represents the time delayed feedback. For small time delay,  $u'_f(t - \tau)$  can be approximated as

$$u'_f(t - \tau) \approx \sum_{j=1}^{\infty} [\eta_j(t) - \tau \dot{\eta}_j(t)] \cos j\pi x_f \quad (5)$$

For simplicity, we consider a single mode for the analysis. The ordinary differential equations obtained after adopting Galerkin technique [32] are given below.

$$\frac{d\eta}{dt} = \dot{\eta} \quad (6)$$

$$\frac{d\dot{\eta}}{dt} + 2\epsilon\omega\dot{\eta} + \omega^2\eta = \dot{Q}' + \xi(t) \quad (7)$$

where  $2\epsilon\omega$  is the damping coefficient and  $\omega = \pi$ . The unsteady heat release rate function is given by

$$\dot{Q}' = -c_1(\eta - \tau\dot{\eta}) - c_2(\eta - \tau\dot{\eta})^3 + c_3(\eta - \tau\dot{\eta})^5 \quad (8)$$

where  $c_1$ ,  $c_2$  and  $c_3$  are constants. It is to be noted that the model captures the experimental results only qualitatively. This is because, the heat release rate expression used in the model does not capture the exact physical conditions in experiments. The expression for heat release rate adopted in the model does not represent the

actual heat transfer rate from a mesh which is the heating element used in the experiments. Further, we neglected the effect of mean flow in the model. These changes bring in the quantitative differences between the model and experiments. Therefore, the values of the parameters that must be maintained in the model are quite different from that in experiments, in order to observe similar dynamical features. We have adopted the specific expression for heat release rate (Eq. (8)) to capture the essential features of a thermoacoustic system. The heat release rate responds to the velocity fluctuations at the heater location after a time delay. Further, the heat release rate provides a nonlinear feedback on the evolution of pressure and velocity fluctuations [21]. In experiments, a subcritical bifurcation to oscillatory behavior is observed as the heater power is varied. A simple way to capture this behavior in the model is to include third and fifth order nonlinear terms in the expression for heat release rate instead of adopting a more general nonlinear function. The constants are chosen such that the bistable behavior observed in experiments can be captured. The model for heat release rate given in Eq. (8) is similar to the functions adopted in earlier studies by Campa & Juniper [33] and Subramanian *et al.* [2]. In Eq. (7), we include a Gaussian white noise term  $\xi$  with  $\langle \xi(t) \rangle = 0$  and  $\langle \xi(t)\xi(t + \tau) \rangle = I\delta(\tau)$  to capture the influence of noise present in the system, where  $I$  is the noise intensity.

### III. RESULTS

The time series of unsteady pressure is acquired from experiments in the presence and absence of external noise for a range of the bifurcation parameter. The heater power is used as the bifurcation parameter in experiments. The median of the peak acoustic pressure  $P$  is non-dimensionalised with the limit cycle amplitude at the Hopf point attained in the absence of external noise ( $P_H$ ) to obtain  $p = P/P_H$ . The heater power  $K$  in experiments is non-dimensionalised with the value of heater power at the Hopf point attained in the absence of external noise ( $K_H$ ). Thus,  $k = 1 - K/K_H$ . The bifurcation diagram between the non-dimensional variables  $p$  and  $k$  is presented in Fig. 2. It is to be noted that the system is not forced with external noise in the case of Fig. 2a. However, there will be inherent fluctuations in the system which must be accounted for. The amplitude of these fluctuations or the noise level in the system is estimated by measuring the rms amplitude of the acoustic pressure when the system is in the non-oscillatory state. Then the noise amplitude is non-dimensionalized by the amplitude of limit cycle attained at the Hopf point in the absence of external noise. The non-dimensional noise intensity  $\alpha$  is estimated to be 0.02 in the absence of external forcing.

A clear hysteresis region or bistable zone can be observed in Fig. 2a. We observe that the width of the bistable zone decreases with increase in the intensity of external noise [23]. Further, in the presence of external

noise of intensity  $\alpha = 0.5$ , the bistable zone gets suppressed as evident from Fig. 2b. The bifurcation points are not discernable in the case of high intensity noise as opposed to the case where external noise is absent. In the presence of fluctuations, multiple realizations are required to describe the transition as any measured observable from the system is a stochastic variable. In this case, the peaks in the time series of acoustic pressure will follow a definite distribution rather than a single value. The transition could be meaningfully described in terms of the nature of the amplitude distribution in such cases. Bifurcations in the system could be observed as changes in the distribution of the amplitude.

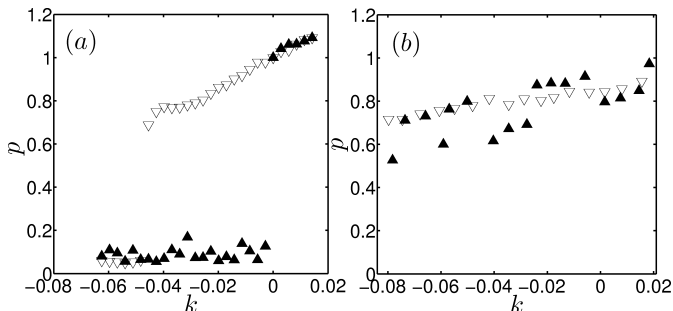


FIG. 2. Bifurcation diagram corresponding to the time series of unsteady pressure obtained from experiments with non-dimensional noise intensity (a)  $\alpha = 0.02$  and (b)  $\alpha = 0.5$ . A significant bistable zone can be observed in (a) where the critical points of transition (Hopf and fold points) are clearly seen. In the presence of high intensity noise, the hysteresis zone is completely suppressed as seen in (b).  $\blacktriangle$ - Increasing  $k$ ;  $\nabla$ - Decreasing  $k$

We intend to obtain the steady state amplitude distribution in three parameter regimes,  $k < k_f$ ,  $k_f < k < k_H$  and  $k > k_H$ , where  $k_f$  and  $k_H$  correspond to the fold and Hopf points of the thermoacoustic system in the absence of external noise. We performed a Hilbert transform of the time series of unsteady pressure to obtain the variation of amplitude and phase with time [34]. A histogram of the amplitudes provides the amplitude distribution for the cases  $k < k_f$  and  $k > k_H$ . In the regime  $k_f < k < k_H$ , the system remains in only one of the two asymptotic states; i.e., either in the non-oscillatory state or in the oscillatory state. However, we require the amplitude distribution, obtained for a parameter chosen in the bistable regime, to capture both the stable states. Therefore, we adopt the following procedure to acquire the time series (of 120 seconds long) of unsteady pressure and develop the amplitude distribution. Initially the parameters are chosen such that the system is in the non-oscillatory state of the bistable regime. The system is given an excitation of amplitude greater than the unstable limit cycle amplitude at the middle of the run for 10 seconds. The frequency of the excitation is same as that of the stable limit cycle. This perturbation transitions the system to the oscillatory state allowable for the same parameter. During this process, we acquire the time se-

ries of fluctuating pressure to capture the non-oscillatory and oscillatory states attained by the system.

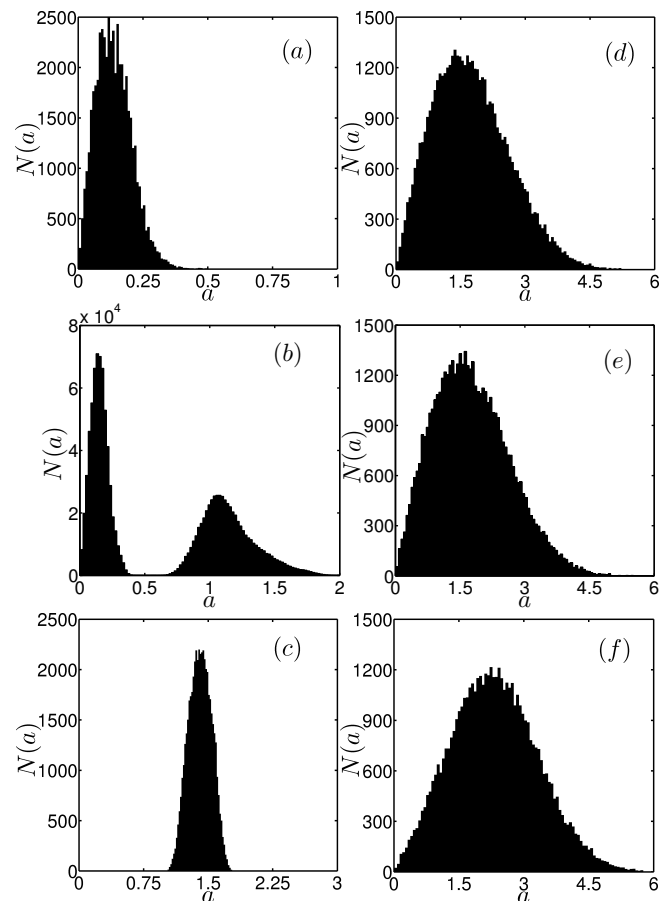


FIG. 3. The left panel shows the distribution of amplitude of acoustic pressure  $N(a)$  in the presence of non-dimensional noise intensity  $\alpha = 0.02$  for (a)  $k < k_f$  (b)  $k_f < k < k_H$  (c)  $k > k_H$ . The right panel shows the distribution of amplitude of acoustic pressure  $N(a)$  in the presence of non-dimensional noise intensity  $\alpha = 0.5$  for (d)  $k < k_f$  (e)  $k_f < k < k_H$  (f)  $k > k_H$ . P-bifurcation is observed as the distribution changes from unimodal to bimodal and then back to unimodal as the parameter is changed in the presence of low intensity noise (left panel). However, the distribution remains unimodal irrespective of the change of control parameter in the presence of high intensity noise as seen in right panel.  $k_f$  and  $k_H$  correspond to parameter values at the fold and Hopf points of the system in the presence of low intensity noise respectively.

The amplitude distributions obtained for the parameter regimes  $k < k_f$ ,  $k_f < k < k_H$  and  $k > k_H$  in the absence (Figs. 3a, 3b, 3c) and presence (Figs. 3d, 3e, 3f) of external noise are shown in Fig. 3. The length of the time series was maintained constant to obtain the amplitude distribution for all the subfigures in Fig. 3 except for Fig. 3b. A longer time series was required for Fig. 3b in order to obtain a smooth distribution. In the absence of external noise, the amplitude distribution changes from unimodal to bimodal and again to unimodal as the parameter is changed. In the presence of

high intensity external noise, the amplitude distribution remains unimodal for all the parameter regimes. Thus, no change in the amplitude distribution is observed in the presence of high intensity noise. To study this behavior of the probability distribution of amplitudes, we derive the Fokker-Planck equation corresponding to Eqs. 6 & 7. The probability distribution is a solution to the Fokker-Planck equation.

### A. Stationary probability distribution from the Fokker-Planck equation

We write the state variables  $\eta$  and  $\dot{\eta}$  (used in Eq. 6 & 7) in terms of slowly varying amplitude and phase [35].

$$\eta(t) = a(t)\cos\theta(t) \quad (9)$$

$$\dot{\eta}(t) = -\omega a(t)\sin\theta(t) \quad (10)$$

where  $\theta(t) = \omega t + \phi(t)$ . We define a parameter  $\beta = 2\epsilon\omega - c_1\tau$ . The term  $\epsilon$  will be absorbed into the parameter  $\beta$  which is subsequently used as the bifurcation parameter. Then, we transform Eqs. (6) & (7) in terms of the new variables  $a(t)$  and  $\phi(t)$ .

$$\frac{da}{dt} = f_1(a, \theta)\sin\theta + g_1(a, \theta)\xi(t) \quad (11)$$

$$\frac{d\phi}{dt} = f_2(a, \theta)\cos\theta + g_2(a, \theta)\xi(t) \quad (12)$$

where,

$$f_1 = -a\beta\sin\theta + \frac{c_1a\cos\theta}{\omega} + \frac{c_2a^3(\cos\theta + \omega\tau\sin\theta)^3}{\omega} - \frac{c_3a^5(\cos\theta + \omega\tau\sin\theta)^5}{\omega} \quad (13)$$

$$f_2 = \frac{f_1}{a}, \quad g_1 = -\frac{\sin\theta}{a}, \quad g_2 = -\frac{\cos\theta}{a\omega} \quad (14)$$

To derive the stochastic equations for  $a$  and  $\phi$ , we perform averaging of Eqs. (11) and (12) over one cycle of oscillation. More details on averaging can be found in Roberts & Spanos [36].

$$da = F_1 dt + \frac{I}{4a\omega^2} dt + \sqrt{\frac{I}{2\omega^2}} dW_1(t) \quad (15)$$

$$d\phi = F_2 dt + \frac{1}{a} \sqrt{\frac{I}{2\omega^2}} dW_2(t) \quad (16)$$

where  $W_1(t), W_2(t)$  are independent Wiener processes and

$$F_1 = \frac{1}{2\pi} \int_0^{2\pi} f_1 \sin\theta d\theta \quad (17)$$

$$F_2 = \frac{1}{2\pi} \int_0^{2\pi} f_2 \cos\theta d\theta \quad (18)$$

Clearly, the equation for amplitude is independent of the phase. Therefore, it is not necessary to write the joint probability density for amplitude and phase. The transition probability density function  $p(a, t)$  for the amplitude can be obtained as a solution of the following Fokker-Planck equation.

$$\frac{\partial p(a, t)}{\partial t} = \frac{\partial}{\partial a} \left[ \left( \frac{\beta a}{2} - \frac{3c_2 n a^3}{8\omega} + \frac{5c_3 m a^5}{16\omega} - \frac{I}{4a\omega^2} \right) p(a, t) \right] + \frac{\partial^2}{\partial a^2} \left[ \frac{I}{4\omega^2} p(a, t) \right] \quad (19)$$

where,  $n = \omega\tau + (\omega\tau)^3$  and  $m = \omega\tau + 2(\omega\tau)^3 + (\omega\tau)^5$ . The stationary probability density  $p(a)$  can be obtained from Eq. (19) as given below.

$$p(a) = C a \exp \left[ -\frac{a^2 \omega^2 \beta}{I} + \frac{3c_2 n \omega a^4}{8I} - \frac{5c_3 m \omega a^6}{24I} \right] \quad (20)$$

where  $C$  is the normalization constant. The extrema of the stationary probability density function  $p(a)$  can be obtained from the roots of the equation given below.

$$8\beta a^2 - \frac{6c_2 n a^4}{\omega} + \frac{5c_3 m a^6}{\omega} - \frac{4I}{\omega^2} = 0 \quad (21)$$

The extrema can be obtained for different values of  $\beta$  and  $I$ , where  $I$  is the intensity of additive noise. The number of real roots of Eq. (21) indicates the nature of the probability distribution. The distribution is unimodal if the number of real roots is 1 while the distribution is bimodal if the number of real roots is 3 [1].

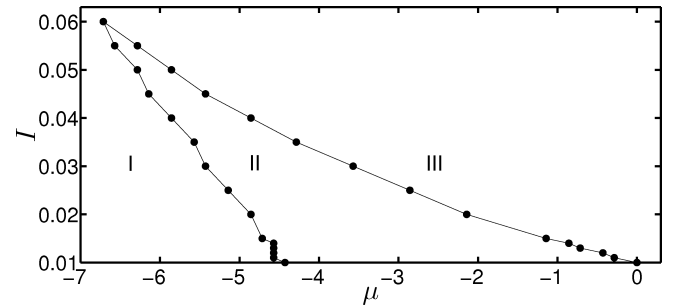


FIG. 4. The regimes of unimodal and bimodal stationary probability distribution in the  $(\mu, I)$  plane, where  $\mu$  is the control parameter and  $I$  is the intensity of the noise. Regions I and III correspond to the parameter regimes where the amplitude distribution is unimodal whereas region II corresponds to the parameter regime of bimodal amplitude distribution. The boundaries of the regions represent the locus of points where P-bifurcation occurs. P-bifurcations are not observed above a noise intensity.

Here, we define a normalized parameter,  $\mu = 1 - \beta/\beta_h$ , where  $\beta_h$  is the value of the parameter  $\beta$  at the Hopf point.

The bifurcation diagram in the  $(\mu, I)$  plane is shown in Fig. 4. Regions I and III correspond to unimodal probability distribution of amplitude while region II corresponds to bimodal amplitude distribution. For low intensities, P-bifurcations can be observed when the parameter  $\mu$  is varied. As the noise intensity is increased, the bimodality region reduces which corresponds to the reduction in width of the hysteresis zone observed in the experiments. Beyond a noise level (noise intensity  $I = 0.06$  in the model), P-bifurcations are not observed. In this case, the probability distribution remains unimodal for changes in the parameter  $\mu$ . The same behavior is observed in experiments for high external noise levels as evident from Fig. 3.

#### IV. DISCUSSIONS

We studied the influence of noise in a thermoacoustic system using the time series of unsteady pressure obtained from experiments and a mathematical model. We observed stochastic P-bifurcations in the system in the presence of noise. In experiments and in the model, a

reduction in the width of the bistable zone is observed with increase in the intensity of external noise. The hysteresis region gets suppressed in the presence of high intensity noise. We used stationary amplitude distribution along with the median of peaks to describe the bifurcation, as the observables are obtained from a noisy system. We identified stochastic P-bifurcations in the system as changes in the stationary probability distribution in the presence of low intensity noise. However, P-bifurcations are not observed in the presence of high intensity noise. Therefore, the noise intensity at which hysteresis region is suppressed corresponds to the regime where P-bifurcations do not exist.

#### ACKNOWLEDGEMENTS

This study is funded by ONR Global (Office of Naval Research Global), USA. We gratefully acknowledge the discussions with Prof. Nicolas Noiray (ETH, Zurich). We also thank Prof. Sayan Gupta (IIT Madras, Chennai) for explaining the concept of P-bifurcations.

- 
- [1] A. Zakharova, T. Vadivasova, V. Anishchenko, A. Koseska, and J. Kurths. *Phys. Rev. E*, **81**:011106, 2010.
  - [2] P. Subramanian, R. I. Sujith, and P. Wahi. *J. Fluid Mech.*, **715**:210, 2013.
  - [3] L. Franzoni, R. Mannella, P. V. E. McClintock, and F. Moss. *Phys. Rev. A*, **36**:834, 1987.
  - [4] O. V. Ushakov, H.-J. Wünsche, F. Henneberger, I. A. Khovanov, L. Schimansky-Geier, and M. A. Zaks. *Phys. Rev. Lett.*, **95**:123903, 2005.
  - [5] P. M. Geffert, A. Zakharova, A. Vüllings, W. Just, and E. Schöll. *Eur. Phys. J. B*, **87**:1, 2014.
  - [6] V. Semenov, A. Feoktistov, T. Vadivasova, E. Schöll, and A. Zakharova. *Chaos*, **25**:033111, 2015.
  - [7] I. Bashkirtseva, T. Ryazanova, and L. Ryashko. *Phys. Rev. E*, **92**:042908, 2015.
  - [8] R. L. Stratonovich. *Topics in the theory of random noise, Volume 2*. Gordon and Breach, New York, 1967.
  - [9] H. Risken. *The Fokker-Planck Equation: Methods of Solution and Applications*. Springer, Berlin, 1989.
  - [10] C. W. Gardiner. *Handbook of stochastic methods*. Springer, Berlin, 1997.
  - [11] L. Arnold. *Random Dynamical Systems*. Springer, Berlin, 2003.
  - [12] Y. Xu, R. Gu, H. Zhang, W. Xu, and J. Duan. *Phys. Rev. E*, **83**:056215, 2011.
  - [13] S. R. D. Djeundam, R. Yamapi, T. C. Kofane, and M. A. Aziz-Alaoui. *Chaos*, **23**:033125, 2013.
  - [14] C. Song, H. Phenix, V. Abedi, M. Scott, B. P. Ingalls, M. Krn, and T. J. Perkins. *PLoS Comput. Biol.*, **6**:e1000699, 2010.
  - [15] L. Billings, I. B. Schwartz, D. S. Morgan, E. M. Bollt, R. Meucci, and E. Allaria. *Phys. Rev. E*, **70**:026220, 2004.
  - [16] V. S. Anishchenko, T. E. Vadivasova, A. V. Feoktistov, V. V. Semenov, and G. I. Strelkova. Experimental studies of noise effects in nonlinear oscillators. In *Nonlinear Dynamics and Complexity*, pages 261–290. Springer, 2014.
  - [17] R. H. Enns and G. C. McGuire. *Nonlinear Physics with Mathematics for Scientists and Engineers*. Birkhäuser, Basel, 2001.
  - [18] S. C. Fisher and S. A. Rahman. *Remembering the giants: Apollo rocket propulsion development*. NASA History Division, Washington, DC, 2009.
  - [19] K. R. McManus, T. Poinsot, and S. M. Candel. *Prog. Energy Combust. Sci.*, **19**:1, 1993.
  - [20] T. C. Lieuwen. *Unsteady Combustor Physics*. Cambridge University Press, Cambridge, UK, 2012.
  - [21] K. Balasubramanian and R. I. Sujith. *Phys. Fluids*, **20**:1, 2008.
  - [22] M. P. Juniper. *J. Fluid Mech.*, **667**:272, 2011.
  - [23] E. A. Gopalakrishnan and R. I. Sujith. *J. Fluid Mech.*, **776**:334, 2015.
  - [24] V. Jegadeesan and R. I. Sujith. *Proc. Combust. Institute*, **34**:3175, 2013.
  - [25] L. Kabiraj, R. Steinert, A. Saurabh, and C. O. Paschereit. *Phys. Rev. E*, **92**:042909, 2015.
  - [26] I. Waugh, M. Geuß, and M. Juniper. *Proc. Combust. Institute*, **33**:2945, 2011.
  - [27] I. C. Waugh and M. P. Juniper. *Intl. J. Spray Combust. Dyn.*, **3**:225, 2011.
  - [28] N. Noiray and B. Schuermans. *Intl. J. Non-Linear Mech.*, **50**:152, 2013.
  - [29] N. Noiray and B. Schuermans. *Proc. R. Soc. A*, **469**:20120535, 2013.
  - [30] K. Matveev. Thermoacoustic Instabilities in the Rijke Tube: Experiments and Modeling. *Phd Thesis*, 2003.

- [31] F. Nicoud and K. Wieczorek. *Intl. J. Spray Combust. Dyn.*, **1**:67, 2009.
- [32] B. Zinn and M. Lores. *Combust. Sci. Technol.*, **4**:269, 1972.
- [33] G. Campa and M. P. Juniper. *Proc. of ASME Turbo Expo*, pages June 11–15, 2012.
- [34] P. F. Panter. *Modulation, noise, and spectral analysis*. McGraw-Hill, New York, 1965.
- [35] N. Kryloff and N. Bogoliuboff. *Introduction to Non-Linear Mechanics*. Princeton University Press, Princeton, 1949.
- [36] J. B. Roberts and P. D. Spanos. *Intl. J. Non-Linear Mech.*, **21**:111, 1986.